Journal of Hazardous Materials 512 (2026) 142357

Contents lists available at ScienceDirect

Journal of Hazardous Materials

journal homepage: www.elsevier.com/locate/jhazmat

Chemical complexity and enrichment in wildland–urban interface fire emissions: A case study of particulate matter, gas-phase pollutants, and ash from the 2025 Los Angeles fires

José Guillermo Cedeño-Laurent [a,b,*], Leonardo Calderón [b], Irini Tsiodra [b,c,d,e], Sanjay Pradeep [f], Hope Davey [g], Roxana Rahmati [h], Lila Bazina [a,b], Xianqiang Fu [i], Namuun Batbaatar [i], Candace SJ Tsai [g], Nikolaos Mihalopoulos [c,e], Dibyendu Sarkar [h], Chunrong Jia [i], Mohammed Baalousha [j], Philip Demokritou [a,b]

[a] Department of Environmental and Occupational Health and Justice, Rutgers School of Public Health, Piscataway, NJ 08854, USA
[b] Nanoscience and Advanced Materials Cente, Environmental and Occupational Health Sciences Institute (EOHSI), Rutgers University, Piscataway, NJ 08854, USA
[c] Environmental Chemical Processes Laboratory, Department of Chemistry, University of Crete, Heraklion GR-71003, Greece
[d] Center for the Study of Air Quality and Climate Change, Institute of Chemical Engineering Sciences, Foundation for Research and Technology Hellas, Patras GR-26504, Greece
[e] Institute for Environmental Research and Sustainable Development, National Observatory of Athens, Lofos Koufou, P. Penteli, Athens GR-15236, Greece
[f] Department of Mechanical and Aerospace Engineering, Samueli School of Engineering, University of California, Los Angeles (UCLA), Los Angeles, CA 90095, USA
[g] Department of Environmental Health Sciences, Fielding School of Public Health, University of California, Los Angeles (UCLA), Los Angeles, CA, USA
[h] Department of Civil, Environmental and Ocean Engineering, Stevens Institute of Technology, Hoboken, NJ 07030, USA
[i] School of Public Health, University of Memphis, Memphis, TN 38152, USA
[j] Center for Environmental Nanoscience and Risk, Department of Environmental Health Sciences, Arnold School of Public Health, University of South Carolina, Columbia, SC 29208, USA

HIGHLIGHTS

- WUI fire emissions show chemical profiles distinct from biomass wildfire smoke.
- Ultrafine particles ($PM_{0.1}$) were highly enriched with non-crustal metals.
- PACs and metals exceeded LA background and biomass wildfire levels by orders of magnitude.
- BTEX concentrations during the fire were 4.8–13 × higher than regional background.
- Ash contained PACs, metals, and PFAS, indicating persistent post-fire contamination.

GRAPHICAL ABSTRACT

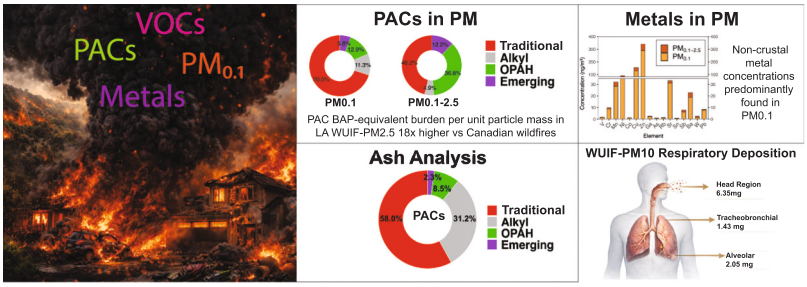

ARTICLE INFO

Keywords:
WUI fires
Wildfires
Ultrafine particulate matter

ABSTRACT

The Los Angeles (LA) wildland–urban interface (WUI) fires of January 2025, are among the most destructive natural disasters in U.S. history, generating complex emission profiles that remain insufficiently characterized. An intensive field sampling campaign was conducted during the active burn period to collect and characterize the complex physicochemical properties of size-segregated particulate matter (WUIF-PM), vapor-phase

* Corresponding author at: Department of Environmental and Occupational Health and Justice, Rutgers School of Public Health, Piscataway, NJ 08854, USA.
E-mail address: memo.cedeno@rutgers.edu (J.G. Cedeño-Laurent).

https://doi.org/10.1016/j.jhazmat.2026.142357
Received 6 March 2026; Received in revised form 20 April 2026; Accepted 8 May 2026
Available online 10 May 2026
0304-3894/© 2026 The Authors. Published by Elsevier B.V. This is an open access article under the CC BY-NC license (http://creativecommons.org/licenses/by-nc/4.0/).

PAHs
LA Fires

compounds (WUIF-VOC), and ash (WUIF ash). While regulatory air quality indices remained within moderate categories during the sampling period, chemical analyses revealed substantial enrichment of hazardous species relative to urban background and biomass-only wildfire conditions. Oxygenated and highly toxic polycyclic aromatic hydrocarbons (OPAHs) were found in ultrafine WUIF-$PM_{0.1}$, (size < 100 nm) and the fractional concentration (μg/g) of US EPA 16 priority polycyclic aromatic hydrocarbons (PAHs) in WUIF-$PM_{2.5}$ exceeded recent levels for LA background, and biomass-only wildfires by an order of magnitude due to the excessive burn of human-made structures. Non-crustal metals were predominantly concentrated in WUIF-$PM_{0.1}$ and consistently enriched relative to both LA background (up to ~30 ×) and biomass-only wildfire aerosols (10–1000 ×). Benzene, toluene, ethylbenzene, and xylene (BTEX) concentrations in WUIF-VOC air samples were 4.8–13-fold higher than background levels. More alarmingly, WUIF ash samples contained PAHs, metals, and per- and polyfluoroalkyl substances (PFAS) consistent with mixed combustion of structural materials and vegetation raising concerns for post-fire environmental health risks. These findings indicate that $PM_{2.5}$ mass and criteria air pollutants alone may underestimate the toxicological burden of WUI smoke, and expanded physicochemical monitoring and characterization is needed to advance exposure assessment and health risk evaluation during complex WUI fire events.

1. Introduction

Wildland–urban interface (WUI) fires have emerged as a pressing environmental and public health concern, driven not only by climate change but also by the rapid expansion of human development into fire-prone landscapes [1]. Wildland-urban interface area has expanded at global level due to urbanization, increasing the proportion of wildfires that intersect populated areas and intensifying human exposure [2,3]. Although trends in WUI fire frequency vary geographically, the fraction of fires occurring in WUI zones and the rates of building destruction have risen, reflecting growing structural vulnerability and more consequential public health, environmental and economic impacts [4]. Extreme weather -driven projections further indicate that fire intensity, measured by fire radiative power, is likely to increase across most fire-prone WUI regions under near-term warming scenarios [5]. Contemporary WUI fires are increasingly characterized by greater exposure, higher damage potential, and escalating intensity, underscoring the urgent need to better understand their environmental and health impacts.

Prior WUI fire disasters have highlighted both insights and knowledge gaps regarding emission characteristics from mixed fuel sources. The December 2021 Marshall Fire swept through suburban neighborhoods on Boulder County, Colorado, destroying over 1000 homes in a matter of hours. This blaze, which ignited natural vegetation and hundreds of structures, produced smoke and ash enriched in toxic constituents like polycyclic aromatic compounds (PACs), volatile organic compounds (VOCs), heavy metals (e.g., lead, arsenic), and other combustion byproducts in smoke affected homes [6,7]. Likewise, the August 2023 Lahaina Fire in Hawaii rapidly burned through wildland grasses into an urbanized town, leveling thousands of buildings and leaving behind ash with elevated concentrations of heavy metals from building materials [8].

Wildland-urban interface (WUI) fires, such as the 2025 LA Fires, involve a diverse array of fuels, from trees and shrubs to homes, vehicles, and infrastructure, which burn under highly variable combustion temperatures and oxygen conditions. This heterogeneous fuel and combustion environment produces multiphase emissions, including particles, gases, and ash, with chemical profiles that can differ substantially from purely vegetative wildfires [9]. Wildfire smoke is itself a complex mixture, with particulate matter spanning the fine (0.1–2.5 μm) and ultrafine nanoscale (<100 nm) ranges [9–11]. The nanoscale fraction is especially compositionally complex and dominated by organic carbon (>97%), including PACs and a wide array of toxic organics [10,12–14]. In WUI fires, the addition of anthropogenic materials can further broaden this chemical mixture to include co-emitted hazardous pollutants such as acid gases and cyanide, carcinogenic VOCs (e.g., benzene and formaldehyde), dioxins and furans, and metal-containing aerosols [12,15–20]. Many of these species are also present in biomass burning but occur in different combinations and relative abundances, yielding PM and ash profiles that differ from those of biomass-only wildfires and may have distinct toxicological relevance [16,21].

WUI emissions include toxic organics and co-emitted hazardous pollutants (e.g., cyanide and acid gases, carcinogenic VOCs such as benzene and formaldehyde, dioxins and furans, and metal aerosols) suggesting that WUI fire-derived PM (WUIF-PM) and ash (WUIF ash) may be more toxic than urban background PM or PM and ash from biomass-only wildfires [17,22].

A substantial epidemiologic and toxicologic literature, largely based on biomass-dominated wildfire events, suggests that wildfire smoke exposure is associated with significant health effects. Increases in wildfire-specific $PM_{2.5}$ ($WFPM_{2.5}$) that have been linked to surges in respiratory hospital admissions [23,24] and mental health emergency department visits [25], with mixed or inconclusive evidence for cardiovascular outcomes [26,27]. Toxicological investigations provide mechanistic support for these observations [28,29], and beyond acute impacts, chronic wildfire smoke exposure has been associated with increased odds of mortality [30]. Consistent with this evidence base, our own studies using laboratory-generated WFPM produced with the Wildfire Simulator (WiFS) show that $WFPM_{2.5}$ is considerably more toxic [31–34], and associated with greater adverse health effects [35,36], than $PM_{2.5}$ from other anthropogenic sources, underscoring the importance of composition beyond PM mass alone. However, whether and to what extent these established wildfire-related risks are amplified in WUI fires remains less well understood, because the inclusion of burned structures and consumer materials can alter the physicochemical properties and toxicity of PM and ash. Comprehensive physicochemical and toxicological characterization of WUI-derived particulate matter, gas-phase pollutants, and ash is therefore essential to support risk assessment and guide exposure mitigation.

The January 2025 Los Angeles County WUI Fires provided a stark example of a modern WUI disasters, with extensive losses across both natural and built environments and major societal and economic implications. Two major fires broke out amidst unusually strong Santa Ana winds and drought conditions: the Eaton Fire in the San Gabriel Mountain foothills (affecting Altadena/Pasadena) and the Palisades Fire in the Santa Monica Mountains (affecting Pacific Palisades/Malibu). Both fires combined burned over 37,000 acres and destroyed more than 18,000 homes and structures that generated more than 4.5 million tons of ash and debris [37]. At least 29 fatalities were attributed to the Los Angeles Fires, and tens of thousands of residents were displaced during mandatory evacuations.

In response to the Los Angeles WUI Fires, we conducted an intensive field sampling campaign during the active burn phase to characterize the physicochemical properties of emitted particulate matter (WUIF-PM), co-emitted gases, and residual ash. The primary objective of this study was to comprehensively characterize the composition of the Los Angeles WUI Fire emissions and to contextualize these emissions against (i) Los Angeles urban emissions, (ii) previously reported biomass-only

wildfires emissions, and (iii) prior WUI fire emissions. By systematically comparing both concentrations and compositional profiles from urban, wildfire, and WUI fire emissions, we aim to clarify how WUI fire emissions differ from conventional wildfire and urban pollution emissions, and to inform exposure assessment and health risk evaluation in the aftermath of large-scale WUI fire disasters.

2. Methods

2.1. Sampling methods

Detailed descriptions of sampling configuration, calibration procedures, analytical protocols, and quality control measures are provided in the Supplemental Material.

Sampling Site Description. Ambient air and ash sampling were conducted at a residential site in Pasadena, CA, approximately 3.5 kilometers southwest of the Eaton Fire (Fig. 1). Sampling equipment was positioned ~1.5 m above ground level in an unobstructed backyard area. The campaign spanned January 16–22, 2025, during which fire containment increased from 50% to 95%. For contextual comparison, $PM_{2.5}$, PM_{10}, carbon monoxide (CO), and meteorological data were obtained from a EPA Air Quality System (AQS) monitoring station (Los Angeles North Main Street, AQS ID 06–037–1103) 4.3 km southwest from our sampling site. These data were used to evaluate regional pollutant trends and assess the influence of wind speed on $PM_{2.5}$ concentrations.

2.2. Size-fractionated WUI particulate matter

Size-segregated wildland–urban interface particulate matter (termed WUIF-PM; WUIF-$PM_{0.1}$=ultrafine PM below 0.1 μm, WUIF-$PM_{0.1–2.5}$= PM larger than 0.1μm and smaller than 2.5μm; WUIF-$PM_{2.5}$= fine PM below 2.5μm) was collected using three Harvard Compact Cascade Impactors (CCIs) [38]. One sample per WUIF-PM size fraction for each analyte group (i.e PACs and metals) was collected. For metal analysis, the WUIF-$PM_{0.1}$ fraction was captured on a Teflon filter (PTFE membrane disc filter, 2 μm pore size, 47 mm diameter; Pall Corporation, Port Washington, NY), while the WUIF-$PM_{0.1–2.5}$ fraction was collected on a chemically clean polyurethane foam (PUF) substrate for a 12.9-hour period from January 17, 2025, at 22:31 to January 18, 2025, at 11:27. For PAC analysis, WUIF-$PM_{0.1}$ particles were sampled on a prebaked quartz filter (Pallflex Tissuquartz, 47 mm diameter; Pall Corporation, Port Washington, NY, USA), and WUIF-$PM_{0.1–2.5}$ was collected on a chemically clean PUF from January 16, 2025, at 18:20 to January 17, 2025, at 11:13 (total duration of 16.9 h). Particle collection for toxicological analysis (not part of this study) was performed using two CCIs from January 16, 2025, at 18:25 until January 22, 2025, at 14:18, totaling 139.9 h. Additionally, quartz filters for the PAC analysis were also used for elemental and organic carbon analysis (additional information is presented in the Supplemental Material). Field blanks were included for each size fraction to assess potential contamination during sampling and handling, with one blank analyzed per size fraction for PACs and for metals analysis. Flow rates were calibrated and kept at 30 liters per minute with a TSI 4043 H mass flowmeter (TSI, Shoreview, MN, USA), to ensure accurate size separation and volumetric quantification.

Real-Time WFPM Monitoring. A Scanning Mobility Particle Sizer (NanoScan SMPS model 3910, TSI Inc., Shoreview, MN) was used to measure in real-time particle number concentrations in the 10 −420 nm mobility diameter range.

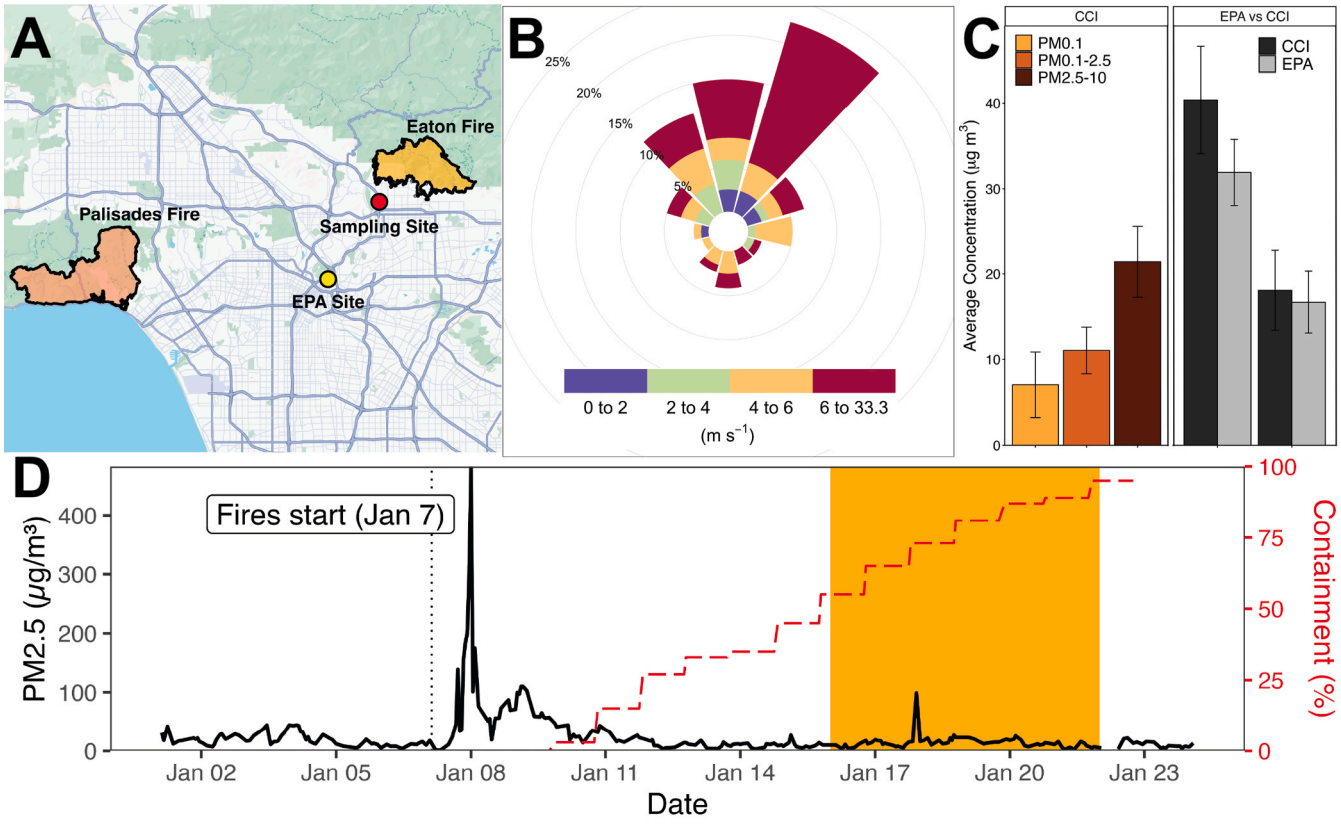

Fig. 1. Particulate matter concentrations during the Los Angeles Fires in January 2026. A) Palisades and Eaton fire perimeters and the location of sampling site and closest Environmental Protection Agency Air Quality System (EPA AQS) site. B) Wind rose frequency plot of direction and wind speed frequency at the EPA AQS site. C) Size-fractionated wildland-urban interface fire-particulate matter (WUIF-PM) mass concentrations during sampling period and comparison to concomitant EPA AQS site values. D) time series plot with $PM_{2.5}$ concentrations from EPA AQS site and average percent containment of the Palisades and Eaton fires (red line); orange area represents the sampling period of our measurements.

WUIF Volatile Organic Compounds (WUIF-VOCs). Ambient WUIF-VOCs were collected using three pre-cleaned stainless steel thermal desorption tubes (Markes International, Bridgend, UK) connected to an SKC Pocket Pump TOUCH (SKC, Eighty Four, PA, USA) operating at a flow rate of 50 mL/min for 80 min. Sampling occurred during two periods: January 16, 2025, at 18:00, and January 17, 2025, at 12:05. One tube served as a field blank. HEPA-Vent filters (Whatman, Wilmington, DE, USA) were employed during sampling to prevent particulate contamination.

WUIF ash Collection. Ash samples (n = 3) were collected from exposed horizontal outdoor surfaces within the WUI area using standardized scraping techniques and contamination-controlled handling procedures. Samples were transferred to sealed containers for laboratory analysis.

2.3. Sample offline physicochemical characterization

2.3.1. Size-specific WUIF-PM mass concentrations

Gravimetric analysis of the size-segregated PM samples was performed using an analytical microbalance (Mettler Toledo, Columbus, OH) to determine time-integrated PM mass concentrations (μg/m^3) by aerodynamic size. All filters and substrates were weighed pre- and post-sampling, with measurements conducted in triplicate (n = 3) after 48-hour conditioning in a temperature- and humidity-controlled environment.

2.3.2. Polycyclic aromatic compounds (PAC) analysis in WUIF-PM and WUIF ash

PAHs and oxygenated polycyclic aromatic hydrocarbons (OPAHs) in WUIF-PM size fractions and ash were analyzed following a protocol adapted from Tsiodra et al. (2024) [39], with full procedural details provided in the Supporting Information. Filters were spiked with deuterated surrogate standards and extracted using accelerated solvent extraction (50:50 n-hexane/dichloromethane), followed by silica column fractionation. The PAC fraction was eluted, concentrated, and amended with an internal standard prior to analysis by GC–MS (Agilent 7890/5975 C, HP-5MS column, full scan mode). Compounds were identified based on retention time, mass spectra, and deuterated analogs, and quantified using daily calibration-derived relative response factors. PACs were classified by type in terms of Traditional (US EPA 16 priority PAHs), Emerging, Alkylated PAHs, and Oxygenated PAHs. A steadily growing body of literature highlights the need to include a broader suite of polyaromatic species, as reliance solely on the Traditional class is recognized to substantially underestimate exposure and associated health risks [40–44].

Benzo[*a*]pyrene-equivalent concentrations (BaP-eq) were calculated to estimate the carcinogenic potency of particulate-associated PAC mixtures by summing the products of compound concentrations and their potency equivalency factors relative to BaP. Two approaches were used: (1) conventional potency equivalency factors (PEFs) for Traditional PAHs following OEHHA/ATSDR guidance to enable comparison with prior studies, and (2) expanded BaP-eq estimates incorporating modeled PEFs from in silico QSAR predictions to include available PEFs for OPAHS, Emerging, and Alkyl PAHs [42].

2.3.3. Metal analysis in WUIF-PM and WUIF ash

The metal concentration in WUIF-$PM_{0.1}$, WUIF-$PM_{0.1–2.5}$, and WUIF ash samples were determined using inductively coupled plasma time-of-flight mass spectrometry (ICP-TOF-MS; TOFWERK, Thun, Switzerland). The elemental composition of individual particles was analyzed using single-particle (SP)- ICP-TOF-MS, following protocols detailed in our earlier work [45–47] and elaborated in the Supporting Information. Elemental ratio distributions were calculated on a per-particle basis, incorporating data from the entire particle population.

2.3.4. WUIF-VOC analysis in ambient air samples

Active and blank TD tube samples were analyzed using a standardized and validated procedure [48]. Each tube was thermally desorbed using an automated TD system (UltraA/Unity2, Markes International, Llantrisant, UK), and the released VOCs were subsequently separated and analyzed using a gas chromatography/mass spectrometry (GC/MS) system (Agilent 7890 A/5975 C; Agilent Technologies Inc., Santa Clara, CA, USA) operated in the scan mode for 84 target compounds (Supplemental Tables S1A and S1B).

2.3.5. Perfluoroalkyl substances analysis in WUIF ash

WUIF ash samples were prepared for PFAS analysis following Liu et al. (2021) [49], with full procedural details provided in the Supporting Information. Briefly, lyophilized and homogenized ash (200 mg) underwent alkaline treatment and ultrasonic methanol extraction, followed by neutralization and centrifugation. Combined extracts were concentrated and purified using Oasis WAX solid-phase extraction cartridges (Waters, Milford, MA, USA). PFAS were eluted, concentrated to near dryness, reconstituted in methanol, filtered (0.22 μm), and spiked with isotopically labeled internal standards (Wellington Laboratories). Quantification was performed using a Waters Xevo UPLC TQ-XS system in accordance with EPA Method 1633.

2.4. WUIF-PM respiratory deposition modelling

Total particle deposition across the human respiratory tract, from head to the alveolar region, was estimated using the Multiple-Path Particle Dosimetry (MPPD) model, version 3.01 developed by Applied Research Associates, Inc [50,51]. The Yeh–Schum symmetric lung model [52] was used assuming a functional residual capacity (FRC) of 3300 mL and a head volume of 50 mL. This model is based on the upright posture exposure to a monodisperse aerosol, characterized by size-specific mass median aerodynamic diameters obtained from the WUIF-PM samples with effective particle densities provided in Table S2. Breathing parameters were set to reflect resting nasal respiration: 12 breaths per minute, 625 mL tidal volume, and an inspiratory fraction of 0.5. The deposited mass was integrated over the 23-day exposure window corresponding to the active fire period.

3. Results and discussion

3.1. Size fractionated WUIF-PM concentrations and influence of meteorological variables

The WUIF-PM mass size distribution measured from gravimetric samples collected between January 16–22, 2025 is shown in Fig. 1c. The mean WUIF-$PM_{2.5}$ mass concentration (18.1 μg/m^3) closely matched the hourly average levels reported by the nearest EPA AQS station at North Main Street (16.7 μg/m^3). Ultrafine WUIF-$PM_{0.1}$ accounted for 40% of the total WUIF-$PM_{2.5}$ mass, a fraction consistent with the high abundance of Aitken-mode particles reported in biomass-burning emissions [11,53]. The mean particle number concentration during Jan 16 sampling was 9181 #/cm^3 (interquartile range (IQR)= 7520–13293 #/cm^3), with a geometric mean mobility diameter of 64.3 nm (IQR=51.7–75.3 nm) (Fig S1). However, we found no prior studies reporting mass-based ultrafine particulate concentrations specifically from WUI fire emissions.

Temporal trends further show that, with the exception of the peak fire period on January 8–9 (WUIF-$PM_{2.5}$ mean= 68 μg/m^3; maximum = 483 μg/m^3), concentrations during the subsequent weeks remained similar to pre-fire conditions and below the NAAQS 24-hour $PM_{2.5}$ standard of 35 μg/m^3. This occurred despite several active fires remaining below 60% containment at the beginning of our sampling campaign and could have been due to the direction of prevailing winds. A sensitivity analysis suggests that strong Santa Ana winds played a significant role in diluting WUIF-PM levels. Winds originating from the

northeast transported emissions offshore, and a linear regression model indicated that each 1 mph increase in wind speed was associated with a 1.2 μg/m^3 decrease in hourly WUIF-$PM_{2.5}$ concentrations, accounting for the containment percentage. These results imply that high wind velocities and wind direction, although contributing to fire spread, substantially reduced local ground-level WUIF-$PM_{2.5}$ burden in urban areas of LA during most of the sampling campaign.

3.1.1. PAC concentrations in WUIF-PM

A total of 47 particulate-phase PACs were detected (40 PAHs and 7 OPAHs), with a total WUIF-$PM_{2.5}$ concentration of 10.6 ng/m^3. Most of this PAC mass was associated with the WUIF-$PM_{0.1–2.5}$ fraction (90.1%; Fig. 2a). Significant differences were observed in the chemical profile of PACs by size fraction. Low molecular weight (LMW; 128–178 g/mol) species dominated the WUIF-$PM_{0.1–2.5}$ fraction (55.5% of PAC mass). In contrast, medium molecular weight (MMW; 202–228 g/mol; 56.9% PAC mass) and high molecular weight species (HMW; 252–300 g/mol; 38.2% PAC mass) together comprised over 95% of PAC mass concentrations in WUIF-$PM_{0.1}$. WUIF-$PM_{0.1}$ was enriched in non-Traditional and highly toxic PAC classes (emerging, alkylated, and oxygenated species collectively representing >50% of PAC mass), whereas WUIF-$PM_{0.1–2.5}$ was dominated by Traditional PAHs (≈70% of PAC mass).

Seven of eight targeted OPAHs were detected in WUIF-$PM_{2.5}$, totaling 1.6 ng/m^3, with 25% of OPAH mass in WUIF-$PM_{0.1}$ (Table S3). 9-Fluorenone and 9,10-anthraquinone were the most abundant species, together accounting for ~70% of the measured OPAHs. These compounds are frequently reported in urban traffic related aerosols and diesel-influenced particulate matter [54,55], and have also been recently found in fresh biomass burning emissions [39]. The presence of multiple higher-molecular-weight ketone/quinone species (e.g., benzo (a)fluorenone and benzanthrone derivatives) is consistent with a mixed WUI source profile that can include high-temperature combustion of structural materials in addition to biomass burning and secondary oxidation of parent PAHs [56].

OPAHs are formed through primary emissions and secondary atmospheric oxidation of their non-oxygenated precursor compounds, commonly referred to as parent PAHs. The ratio of OPAHs to their corresponding parent PAHs is frequently used in source apportionment, as elevated ratios may reflect secondary formation processes, oxidative aging, or differences in combustion conditions. Furthermore, OPAH-to-parent ratios were elevated in WUIF-$PM_{2.5}$ (9-fluorenone/fluorene ≈ 1.0; 9,10-anthraquinone/anthracene ≈ 4.0). While concentration data alone cannot uniquely separate formation pathways, these high ratios are consistent with two non-mutually exclusive mechanisms: (i) direct OPAH emissions during combustion [39] and (ii) secondary production via oxidative transformation of parent PAHs, coupled with dynamic gas–particle partitioning [57–60].

Despite the overall low WUIF-$PM_{2.5}$ mass concentration, our results suggest a substantial enrichment of the particle-bound PAH concentrations relative to previously reported non-fire urban background levels in LA. Aldekheel et al. reported total Traditional PAHs of 0.88 ng/m^3 in $PM_{2.5}$ at an urban Los Angeles site [61]. While this comparison is based on a single urban reference point and does not capture the spatial heterogeneity of the Los Angeles basin, it provides a useful contextual benchmark. Within this context WUIF-$PM_{2.5}$, exhibits nearly an order-of-magnitude increase in the total Traditional PAHs concentration relative to reported urban background levels.

Comparison of fractional PAC concentrations further distinguish the LA WUIF-PM from biomass-based wildfire emitted PM (WFPM). For same PACs species included in both the LA WUIF-PM and the Canadian 2023 WFPM samples the total fractional concentration was 631.9 μg/g in LA WUIF-$PM_{2.5}$, exceeding values reported from the 2023 Canadian wildfire plume impacted New York City metropolitan area [10] (343.3 μg/g). The same hierarchy was observed when comparing the fractional concentration Traditional PAHs between LA WUIF-$PM_{2.5}$: 503.9 μg/g; the Canadian plume: ~69.7 μg/g; and Southern California wildfire samples WFPM [13] ~50 μg/g). The interpretation of this comparison is limited by several factors, including differences in source characterization, sampling proximity to emissions, and the extent of atmospheric processing, and radical oxidation in the case of the Canadian wildfires. Long-range transported wildfire plumes are subject to photochemical transformation (e.g., photolysis, radical oxidation, and volatilization), which can substantially alter their chemical composition relative to the more locally sampled LA WUI Fire emissions.

Compositionally, the WUIF-PM was particularly enriched in LMW PAHs, which were > 6 × higher than in the Canadian wildfire WFPM and ~10 × higher than in Verma's data. In contrast, MMW PAHs were most elevated in the Canadian WFPM, largely driven by high retene levels characteristic of softwood combustion. This LMW-rich particle-phase profile is consistent with relatively fresh biomass-based fire emissions, as laboratory and field observations of plume aging commonly show preferential loss of semi-volatile PAHs through

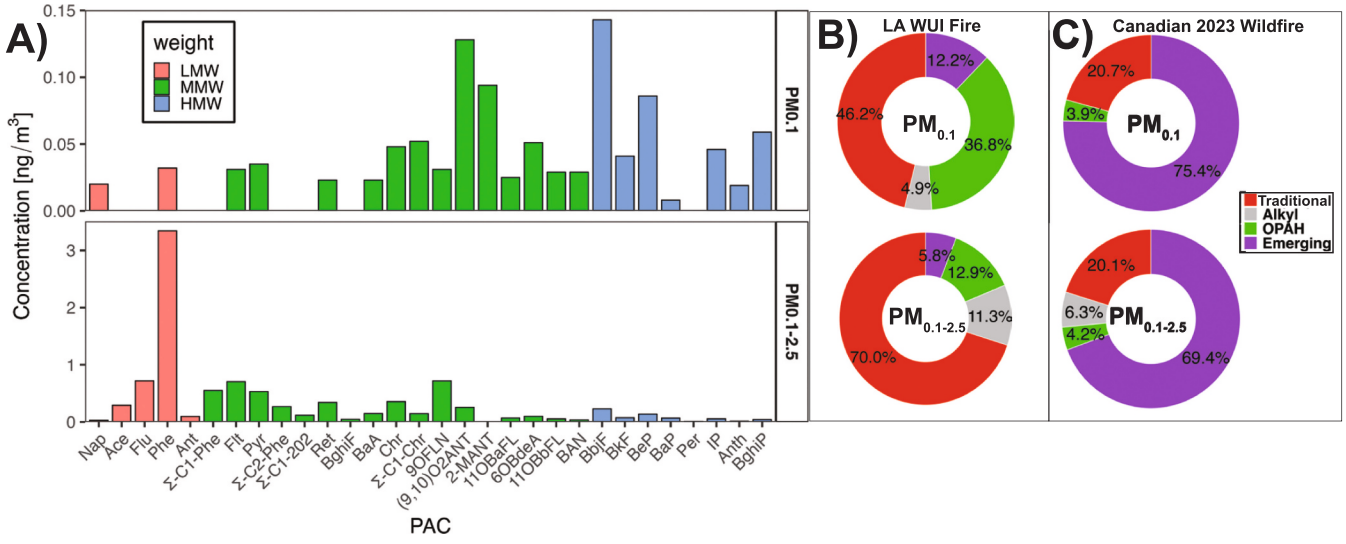

Fig. 2. PAH concentrations in size fractionated wildland urban interface figure-particulate matter (WUI-PM) samples. A) Size-specific concentrations of polycyclic aromatic compounds (PAC) species in WUIF-$PM_{0.1}$ (upper panel) and WUIF-$PM_{0.1–2.5}$ (lower panel) plotted on different y-axis scales for clarity; Distribution of PAC among Traditional, Alkyl, oxygenated and highly toxic polycyclic aromatic hydrocarbons (OPAH), and Emerging categories in $PM_{0.1}$ and $PM_{0.1–2.5}$ from B) Los Angeles WUI fire and C) Canadian 2023 Wildfire from Cedeno-Laurent et al. 2024.

volatilization and oxidation, yielding a relative enrichment of more persistent MMW/HMW PAHs during long-range transport. The LA WUIF-PM composition therefore suggests limited atmospheric processing prior to sampling and additional contributions from non-biomass WUI combustion sources, consistent with the mixed PAC-type composition highlighted in Fig. 2B.

Furthermore, diagnostic PAH ratios further suggest that the particle-phase mixture reflects a complex WUI source profile rather than biomass combustion alone. On one hand, the Flt/(Flt+Pyr) and Ret/(Ret+Chr) ratios of 0.565 and 0.49, respectively, represent values characteristic of biomass or wood combustion [62,63]. On the other hand, the BaA/(BaA+Chr) and IcdP/(IcdP+BghiP) ratios of 0.297 and 0.50, respectively, fell in the mixed-source range, consistent with simultaneous structural material, biomass influence, and local traffic emissions [64,65].

3.1.2. Metal concentrations in WUIF-PM

Metal concentrations showed a strongly ultrafine-dominated mass profile, with WUIF-$PM_{0.1}$ contributing between 75% and 95% to the total WUIF-$PM_{2.5}$ metal content across all detected species (Fig. 3A). The heavy metals with the highest concentrations were zinc, followed by copper, nickel, barium, and lead. WUIF-$PM_{2.5}$ is strongly metal-enriched relative to the historical LA $PM_{2.5}$. Using cold-season (i.e., late fall and winter) $PM_{2.5}$ between 2005 and 2006 [66], geometric mean enrichment factors based on element-specific volumetric concentrations (ng/m^3) for crustal and non-crustal metals are ~3 × (range ~1–60 ×) and ~7 × (range ~2–30 ×), respectively. Relative to decade-mean concentrations collected from 2015 to 2024, the corresponding crustal and non-crustal metal enrichment factors are ~2.2 × and ~30 × [67]. Of particular importance, the LA WUIF-$PM_{2.5}$ lead concentration of 8.4 ng/m^3 is 1.75 × higher than the LA cold-season $PM_{2.5}$ mean concentrations and approximately 4 × higher than the annual 24-hour average concentration measured at the EPA North Street air monitoring station during 2024 [68]. These enrichment ranges match the signal from burnt structural materials, coatings, and electronic components over biomass-dominated wildfire smoke or urban background aerosol [17] and raise serious environmental health concerns.

More interestingly, metals are substantially enriched in WUIF-PM compared biomass-based WFPM, with the most pronounced differences observed in the ultrafine fraction (Fig. 3B Enrichment factors for Ni, Cu, Zn, Cd, Sb, and Pb in LA WUIF-$PM_{0.1}$ relative to biomass wildfire $PM_{0.1}$ range from 100- to 1000-fold [31,69]. In the fine fraction, WUIF-$PM_{2.5}$ remains substantially enriched in metals compared with wildfire $WFPM_{2.5}$ and firefighter-exposure aerosols, with enrichment factors generally in the 10–100-fold range. Crustal elements (e.g., Fe, Mn, V) show only modest enrichment in both ultrafine and fine fractions, whereas non-crustal metals display consistently strong enrichment across all comparison datasets [31,69,70].

Metal nanoparticle profiles from the LA WUI Fire showed pronounced differences from those observed during the Canadian biomass wildfire [10] (Figure S2). Metal particle number concentrations were approximately one to two orders of magnitude higher in LA WUIF-$PM_{0.1}$ than those in the Canadian wildfire $WFPM_{0.1}$. The nanoparticles most elevated in WUIF-$PM_{0.1}$ (i.e., Al, Ti, Fe, Cu, Zn, Ni, Sb, Sn, and Pb) are consistent with high-temperature volatilization–condensation pathways that nucleate metal-rich ultrafine particles during structural combustion. In contrast, the Canadian wildfire $WFPM_{0.1}$ fraction was dominated by Mn, Fe, and Zn, reflecting biomass mineral content and the absence of anthropogenic metal bearing nanomaterials. In WUIF-$PM_{0.1–2.5}$, particle number concentrations were generally lower than those measured during the Canadian wildfire, except for Ni, and W, which remained elevated in the WUI fire plume and are more characteristic of anthropogenic materials than biomass fuel matrices. However, these differences should be interpreted with caution, as the Canadian wildfire plume reflects long-range transport and possibly photoaging, whereas the LA WUI Fire measurements are more source-proximal and freshly generated. As a result, size-selective removal during transport may influence particle number concentrations and size distributions, limiting direct comparability between the two events.

3.1.3. Gaseous phase WUIF-VOC results

Mean WUIF-VOC concentration was 27.5 ppb, with a profile dominated by substituted aromatics and solvent/fuel-related species. The most abundant species are shown in Fig. 4A. Several compounds consistent with biomass burning (e.g., limonene, α-pinene) [71] and traffic and diesel emissions were also detected (long-chain aliphatic VOCs) [72]. Relative to urban background in Central LA (2022; UATMP/NATTS Central LA site), WUIF-VOC concentrations were consistently higher for key aromatics: benzene 1.27 vs 0.27 ppb (~4.8 ×), toluene 4.41 vs 0.57 ppb (~7.8 ×), ethylbenzene 0.92 vs 0.11 ppb (~8.7 ×), total xylenes 6.36 vs 0.48 ppb (~13 ×), and styrene 0.20 vs 0.02 ppb (~10 ×). While there are no existing reports of VOC during WUI fire events, the toluene and benzene concentrations reported in WUIF-VOC from the Marshall fires in Colorado in 2021 10 days after the fire are similar to those in LA WUIF-VOC concentrations here [6].

When compared against biomass-only wildfire smoke from Dickinson et al., 2022, WUIF-VOC results show a distinct shift toward toluene and xylenes [73]. The across-fire mean concentrations were: benzene= 1.63 ppb, toluene= 1.82 ppb, ethylbenzene= 0.39 ppb, and Σ xylenes= 0.94 ppb. In contrast, LA WUIF-VOC had

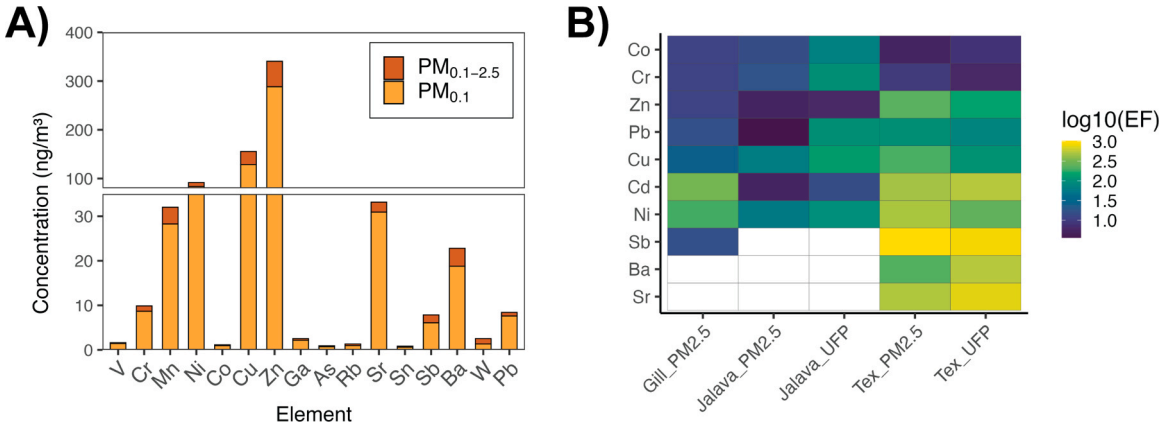

Fig. 3. A Non-crustal metal concentrations in wildland-urban interface-ultrafine and fine particulate matter (WUIF-$PM_{0.1}$ and WUIF-$PM_{0.1–2.5}$, respectively); 3B) metal enrichment factors (EF) in WUIF-$PM_{0.1}$ and WUIF-$PM_{2.5}$ compared with those in biomass-only wildfires (Gill et al. 2024; Jalava et al. 2006) and firefighter exposure monitoring (Tex=Teixeira et al. 2024). Color scale denotes EF on a $\log_{10}$ scale with higher values indicating greater enrichment in WUIF PM relative to the comparison datasets.

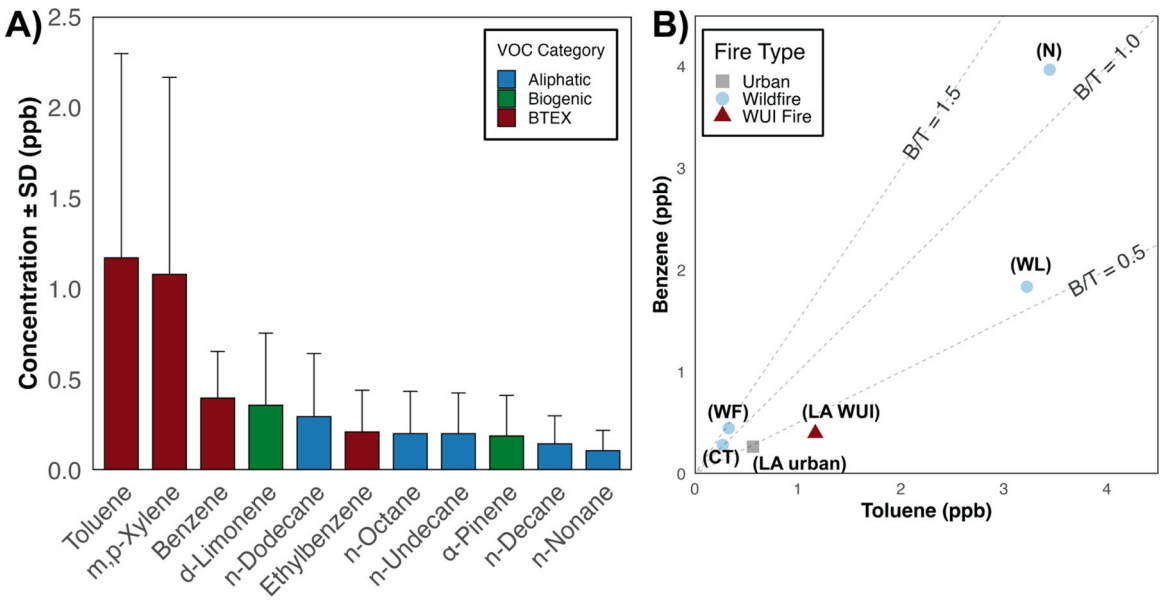

Fig. 4. Volatile organic compounds (VOC) concentrations in vapor phase. A) Mean VOC concentrations (n = 3) by category; B) Comparison of Toluene/Benzene between Los Angeles wildland-urban interface Fire (LA WUIF), Los Angeles urban emissions and wildfire emissions reported by Dickinson et al. 2022: (CT)= Chief Timothy Fire; (WF)=Williams Flats Fire; (WL)=Whitetail Loop Fire; (N) Nethker Fire.

similar-to-slightly-lower benzene (1.27 ppb; ~0.78 × biomass-only) but substantially higher toluene (4.41 ppb; ~2.4 ×), ethylbenzene (0.92 ppb; ~2.3 ×), and Σ xylenes (6.36 ppb; ~6.8 ×). This pattern is also captured by diagnostic ratios: benzene/toluene (B/T) in WUIF-VOC was 0.29, whereas biomass-only fires clustered around ~1 (Dickinson fire-specific B/T spanning roughly 0.57–1.35; Fig. 4B). Likewise, LA WUIF-VOC Σxylenes/benzene was ~5.0 versus ~0.64 across the biomass-only fires. Although this shift is consistent with added contributions from mixed urban materials and fuel/solvent sources, aromatic emissions are also sensitive to combustion conditions [11,22]. In biomass burning, the balance between flaming and smoldering combustion can strongly influence VOC composition, with aromatic hydrocarbons enriched in the high-temperature profile and aromatic oxygenates and furans enriched in the low-temperature profile [74]. WUI fire surrogate burns further show that reduced oxygen availability and ventilation can increase non-methane organic compound (NMOG) yields, and that synthetic polymer combustion is an important source of reduced cyclic aromatics such as benzene and styrene [75]. Because modified combustion efficiency (MCE), an indicator of combustion conditions [76], could not be estimated for our field samples, we cannot resolve the relative contributions of fuel composition versus combustion conditions to the observed aromatic enrichment. We therefore interpret the elevated toluene, ethylbenzene, and xylenes as consistent with, but not uniquely diagnostic of, mixed urban material combustion

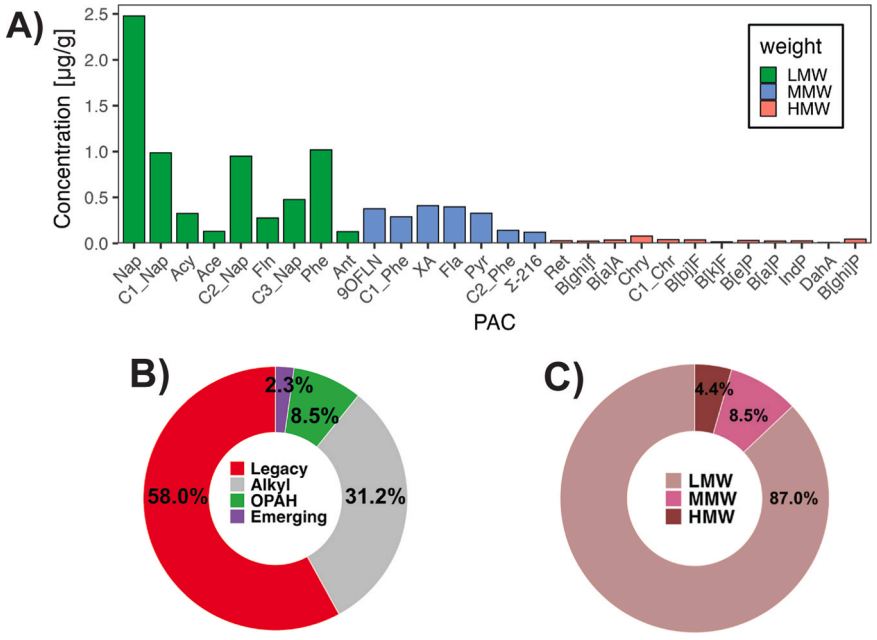

Fig. 5. Polycyclic aromatic carbon (PAC) concentrations in wildland-urban interface fire (WUIF) ash. A) Concentrations in ug g^{-1} for individual species; B) Percent contribution of total PAC mass by PAC category, including the Traditional, Alkyl, Oxygenated and highly toxic polycyclic aromatic hydrocarbons (OPAH), and emerging; and C) by molecular weight (Low molecular weight=LMW; Medium molecular weight=MMW; High molecular weight=HMW).

superimposed on biomass burning and local background sources.

3.1.4. PACs in WUIF ash

Twenty-eight PACs were detected in LA WUI ash, including 26 PAHs and 2 OPAHs (Figs. 5A and 5B). PACs in LA WUIF ash were dominated by LMW species (87% of total parent PAC mass) and the Traditional PAHs comprised the dominant fraction of quantified PACs in ash (Fig. 5C). Emerging OPAHs and alkyl PAHs were also detected. However, their levels were in a reduced proportion by mass compared to species found in airborne PM. Recent experimental work simulating WUI fire emissions has shown that OPAHs can be preferentially formed in mixed fuel systems containing both biomass and synthetic materials (e.g., HDPE plastic), compared to biomass-only combustion [21], supporting their potential association with the combustion of human-made structures. However, OPAHs and alkylated PAHs can also originate from other sources such as traffic emissions and their presence in WUIF ash could reflect contributions from pre-existing urban dust [54].

Furthermore, WUIF ash PAH concentrations were compared to PAH concentrations from wildfire ash values reported by Yang et al., from compiled forest fire ash across 51 sites globally [77]. The mean total PAH concentration from the Traditional PAHs in forest fire ash was 1322 ng/g, whereas the corresponding total in the LA WUIF ash was 5363 ng/g, indicating approximately fourfold enrichment in the WUIF samples. This amplification was consistent across individual compounds, with most parent PAHs elevated by three to ten times relative to the forest fire ash average (Table S4).

PAH diagnostic (molecular) ratios are dimensionless ratios of selected PAH isomers (e.g., Flt/(Flt+Pyr), Ant/(Ant+Phe)) that are commonly used as first-order, qualitative indicators of dominant PAH sources because different fuels and combustion conditions produce characteristic isomer patterns [78]. Wildfire-ash reference ratios used here are drawn from the Yang et al. compilation (a meta-analysis synthesizing post-fire PAH datasets from 51 burned areas globally). Despite large differences in absolute concentrations, two widely used combustion indicators were nearly identical between the LA WUIF ash and the average ratios from the Yang et al. compilation [77]: Flt/(Flt+Pyr) was 0.56 in wildfire ash and 0.55 in WUIF ash, and Ant/(Ant+Phe) was 0.12 and 0.11, respectively—values consistent with pyrogenic/biomass-combustion signatures (Flt/(Flt+Pyr) > 0.5; Ant/(Ant+Phe) > 0.1). In contrast, IcdP/(IcdP+BghiP) decreased from 0.532 (wildfire ash) to 0.381 (WUIF ash), shifting from the biomass/coal-combustion regime (>0.5) toward the petroleum-combustion/mixed-source range (0.2–0.5) and indicating a relative enrichment of benzo[*g*,*h*,*i*]perylene in the WUIF ash. This divergence is consistent with the more compositionally complex fuel mix typical of WUI fires, where burning of structural and petroleum-derived materials can contribute additional PAH signatures beyond biomass alone [79].

3.1.5. PAC BaP-eq calculations for the LA WUIF-PM and WUIF ash

BaP-equivalent (BaP-eq) concentrations were calculated for $PM_{2.5}$ using both (i) the OEHHA-based approach applied to Traditional PAHs and (ii) an expanded set of QSAR-derived potency factors [42]. Despite substantially lower WUIF-$PM_{2.5}$ mass during the WUI-LA Fire (18.1 μg/m^3) compared with the Canadian wildfire WFPM (330 μg/m^3), the WUIF-$PM_{2.5}$ BaP-eq concentrations using the OEHHA/EPA approach were nearly identical (0.164 ng /m^3 for LA WUIF-$PM_{2.5}$ vs 0.161 ng /m^3 for the Canadian wildfire WFP$M_{2.5}$). Using the Li et al. (2023) potency factors, BaP-eq remained comparable, with WUIF-$PM_{2.5}$ within ~20% of the Canadian wildfire value (0.568 vs 0.680 ng /m^3 respectively). These results indicate a markedly higher toxicity-weighted PAH burden per unit particle mass in LA WUIF-$PM_{2.5}$ compared to the Canadian wildfire WFP$M_{2.5}$ (~18-fold higher). Relative to urban background conditions in Los Angeles, WUIF-$PM_{2.5}$ BaP-eq was also elevated. Aldekheel et al. reported BaP-eq ≈ 0.1 ng/m^3 in urban LA $PM_{2.5,}$ whereas WUIF-$PM_{2.5}$ BaP-eq under the OEHHA/EPA approach was ~0.164 ng /m^3, representing an increase of approximately ~50–60% during the WUI episode. Additionally, size-resolved results show that this toxicity-weighted enrichment is not evenly distributed across the particle population. Although WUIF-$PM_{0.1}$ contributed only ~10% of total particulate PAC mass, it accounted for 21% of total BaP-eq under the OEHHA/EPA approach and 28% under the Li et al. (2023) framework, indicating a disproportionately high BaP-eq burden per unit PAC mass in ultrafine particles. This enrichment is consistent with the preferential association of more chemically potent PAHs with the ultrafine fraction [10].

For LA WUIF ash, total BaP-eq concentrations were 219 ng/g using the Li et al. PEFs and 55 ng/g using the OEHHA/EPA approach, indicating substantial sensitivity of BaP-eq magnitude to the selected potency framework. This difference was driven primarily by dibenzo[*a*,*h*]anthracene, which was detected in ash but not observed in PM and carries a much higher potency weighting under the Li framework (PEF=10). Dibenzo[*a*,*h*]anthracene is a high potency carcinogenic PAH classified by the International Agency for Research on Cancer (IARC) as probably carcinogenic to humans (Group 2 A), while the EPA relative potency factor guidance places it at parity with BaP. Beyond dibenzo[*a*,*h*]anthracene, the increase in BaP-eq under the Li framework was further amplified by higher PEFs assigned to fluoranthene, benzo(b+j)fluoranthene, and chrysene, with additional contributions from benz[*a*]anthracene and benzo(k)fluoranthene, and OPAHs. However, assigned BaPeq PEF values for OPAHs are novel estimations based on limited toxicological data. Only a subset of the detected OPAHs currently have assigned PEFs, and therefore, the calculated BaPeq does not fully capture the total toxic impact of OPAHs.

3.1.6. Metals in WUIF ash

Crustal elements (Fe, Al, Mg, Ca, Ti, and Si) accounted for most of the inorganic mass (approx. 98%). These major elements were accompanied by a broad array of trace and minor metals, including Mn, V, Ni, Co, Cu, Zn, As, Ba, La, Ce, and Pb, as well as detectable Ga, Sr, Y, Zr, Nb, Sn, Pr, and Nd, spanning roughly three orders of magnitude in concentration (Fig. S3).

Compared with ash from the 2020 North Complex and LNU Lightning Complex WUI fires, the LA WUIF ash shows trace metal concentrations similar to soil samples, with most elements at the lower end of the reported ranges by Alsheri et al., 2023 [47]. Copper, Zn, and Pb were one to two orders of magnitude lower than the median values reported by Alshehri et al., whereas V, Mn, Ni, and Co were near the reported medians, suggesting similar contributions from alloy steels, lubricants, and other metallic components associated with vehicles and residential infrastructure.

Sn, Pb, and Ba represent an additional compositional group suggestive of thermal decomposition of automotive and electronic materials. Sn and Pb are principal constituents of solder alloys and electrical connectors, whereas Ba serves as a filler in brake pads and pigments. The co-occurrence of these three elements mirrors the pattern identified by Alshehri et al. in vehicle ashes, where Sn- and Pb-bearing incidental nanomaterials (INMs) were observed. The presence of As and Zn suggests contributions from multiple potential sources, including anthropogenic materials and regional background composition. Arsenic and zinc may derive not only from treated materials such as legacy chromated copper arsenate in structures [45,80], but also from geogenic enrichment [81] and activities such as mining and agriculture, which are known to influence metal distributions in parts of California [82]. Similarly, Zn may reflect inputs from corrosion-resistant materials and tire-derived particles but can also be present in urban and regional background dust [83].

The presence of Ga, Y, La, Ce, Pr, and Nd reveals a growing electronic and rare-earth elements (REE) signature in modern municipal solid waste incinerators ashes [84]. These elements are key components of semiconductors, phosphors, and Nd–Pr–Fe–B permanent magnets used in lighting, motors, and appliances, suggesting that the combustion of

consumer electronics and vehicles may have contributed to the LA WUIF ash composition. While source attribution remains uncertain, the presence and enrichment of these metals in WUIF ash is of relevance given their deposition near residential environments. The potential for mobilization, resuspension, and direct human contact with ash underscores their importance from an exposure and public health perspective.

3.1.7. PFAS levels in WUIF ash

Twenty-eight out of 40 targeted Per- and polyfluoroalkyl species (PFAS) were detected in the LA WUIF ash samples (n = 3, Table S5). Total PFAS concentrations (ΣPFAS) ranged from 60.5 to 205.8 ng/g (mean: 112.7 ng/g; median: 71.8 ng/g). Detected species were grouped into six compound classes (Fig. S4). Fluorotelomer sulfonates accounted for the majority of ΣPFAS, followed by short-(C4–C7; primarily PFHxA and PFBA) and long-chain (C8–C14; all mean concentrations <2 ng/g) perfluoroalkyl carboxylic acids (PFCAs). Ether-based PFAS represented 6.6% of total mass, followed by perfluoroalkyl sulfonates (PFSAs), sulfonamide precursors (1.0%), and fluorotelomer carboxylic acids (FTCAs).

6:2 FTS, the dominant species in the WUIF ash profile, is used in consumer and building materials [85] and in fluorotelomer-based aqueous film-forming foams (AFFFs) [86]. In WUI fire contexts, both source categories are plausible; however, several lines of compositional evidence favor a predominantly built-environment origin: the co-detection of ether-based replacement PFAS (HFPO-DA, PFEESA, NFDHA, ADONA), which are associated with post-2009 fluoropolymer processing aids in consumer and construction materials [87,88], and the absence of PFHxS, a hallmark of electrochemical fluorination–derived legacy AFFFs. Together, these observations suggest that combustion of PFAS-containing structural and consumer materials was the primary source of the observed fluorotelomer signature, though secondary contributions from firefighting activities cannot be excluded.

Short-chain PFCAs were consistently present at higher concentrations than long-chain homologues. This pattern may reflect the use of short-chain chemistries in post-2006 materials, transformation of fluorotelomer precursors during combustion, or both [89]. FTCAs (3:3 FTCA, 7:3 FTCA), detected at low concentrations, are reported intermediates in fluorotelomer degradation pathways [87] but may also occur as residual impurities in commercial products. The present data do not distinguish among these mechanisms.

Because the samples represent transported ash, the PFAS composition likely integrates inputs from multiple burned structures and landscapes and may reflect enrichment in fine ash fractions [90,91]. Reported concentrations represent targeted PFAS only; side-chain fluorinated polymers and other non-target fluorinated compounds were not quantified and may contribute to total organic fluorine.

3.1.8. WUIF-PM respiratory deposition modeling

WUIF-PM mass deposition in the human airway was estimated using the MPPD model over the 23-day duration of the Palisades and Eaton fires in the LA metropolitan area (Fig. S5). Size-specific concentrations were derived from the integrated sample size distribution and average PM_{10} concentrations measured at the EPA LA North Main Street station. Total inhalable WUIF-PM_{10} respiratory deposition was 9.83 mg, of which 36.3% corresponded to the ultrafine fraction. This total inhalation dose was 7.43% higher than the estimated 9.15 mg dose during the 3-day air quality advisory in the US Northeast following the 2023 Canadian wildfires [10]. Moreover, after accounting for chemical enrichment, the toxicological burden is expected to increase substantially. This is also indicative of the case of PAHs and the BaP-eq calculations presented in previous section. More specifically, the Traditional PAH total BaP-eq dose during the LA WUI episode was 4.6-fold higher than that estimated for the biomass-based Canadian wildfire PM in the New York area. Although estimating lifetime risk and health impact due to PM-bound PAH levels will require mechanistic toxicological studies, emerging data from simulated WUI fires on impact on respiratory health point to impact on lung effects and innate immune function [21].

3.1.9. Strengths, limitations, and implications for future research

This work provides a physicochemically resolved snapshot of a major urban WUI fire episode using measurements of size-fractionated PM, co-occurring gases, and transported ash, shedding light on potential environmental health implications. The findings highlight the chemical complexity of WUI fires, and their comparison to biomass-based fires suggests the potential for increased environmental and public health risks. A central finding is that $PM_{2.5}$ mass concentration metric alone does not adequately capture the toxicological burden associated with WUI chemical complexity. Even when $PM_{2.5}$ mass levels were relatively low for much of the LA WUI fire episode, multiple particle- and gas-phase constituents exceeded orders of magnitude the fractional concentrations in baseline LA pollution and previously documented wildfire events. The complexity in chemical composition supports an unambiguous structural-combustion signature that is readily distinguished from both biomass smoke and LA urban background, even at similar $PM_{2.5}$ mass concentrations. The presence of highly toxic compounds such as emerging PAHs, PFAS, toxic metals found in both the WUIF-$PM_{2.5}$ and WUIF ash raise serious concerns for potential environmental health implications.

This study has several limitations. The limited number of samples, with one sample per analyte group, restricts spatiotemporal resolution and limits the generalizability of our findings beyond the specific collection period and location. In addition, while samples were collected during the active fire period, they missed the peak exposure window of Jan 8–9. Nonetheless, it has been shown that during our sampling period, health service utilization remained elevated despite AQI returning toward baseline [92].

The compositional enrichment of WUIF-PM with highly toxic compounds reinforces the need for composition-informed air pollution exposure metrics [93], particularly for WUI fires in densely populated regions where $PM_{2.5}$ peaks may be brief and below the NAAQS mass-based $PM_{2.5}$ standard.

Important knowledge gaps remain for emerging contaminants such as PACs (e.g., oxygenated and substituted species), and the complex mixtures of multi-phase pollutants, for which toxicological benchmarks and health-relevant dose metrics are limited; mechanistic toxicological studies and integration of real world WUIF-PM hazard characterization data into risk-relevant frameworks are priority needs.

The ash burden, measured on the order of millions of tons deposited across communities, creates a plausible pathway for prolonged exposure via resuspension and indoor migration, contamination of surface waters and edible plants, extending potential inhalation contact beyond the active fire period and increasing the importance of ash physicochemical characterization for remediation planning. Finally, the LA episode's extended duration (≈23 days), despite only a few high-PM days, motivates future work that focuses on potential synergistic health implications from pollutants from other anthropogenic sources such as traffic.

Environmental implications

The chemical composition of emissions from the 2025 Los Angeles WUI fires indicates that environmental contamination extends beyond traditional wildfire impacts and includes pollutants associated with the combustion of urban infrastructure. Elevated concentrations of particle-boundtoxic polycyclic aromatic hydrocarbons, non-crustal metals, BTEX compounds, and PFAS in ash suggest that these fires mobilize complex mixtures of contaminants capable of persisting in air, soil, and indoor environments during recovery. The enrichment of hazardous species in ultrafine particles further increases the potential for long-range transport and human exposure. Together, these findings indicate that conventional air quality indicators may underestimate environmental hazards associated with WUI fires and highlight the need for expanded monitoring and post-fire environmental management strategies.

CRediT authorship contribution statement

Lila Bazina: Writing – review & editing, Writing – original draft, Formal analysis. **Roxana Rahmati:** Writing – review & editing, Formal analysis. **Namuun Batbaatar:** Writing – review & editing, Formal analysis, Data curation. **Xianqiang Fu:** Writing – original draft, Formal analysis, Data curation. **Candace SJ Tsai:** Writing – review & editing, Writing – original draft, Investigation, Formal analysis, Data curation. **Dibyendu Sarkar:** Writing – review & editing, Writing – original draft, Formal analysis, Data curation. **Cedeño-Laurent Jose Guillermo:** Writing – review & editing, Writing – original draft, Visualization, Validation, Supervision, Software, Resources, Project administration, Methodology, Investigation, Funding acquisition, Formal analysis, Data curation, Conceptualization. **Nikolaos Mihalopoulos:** Writing – review & editing, Writing – original draft, Formal analysis, Data curation. **Irini Tsiodra:** Writing – review & editing, Writing – original draft, Investigation, Formal analysis. **Mohammed Baalousha:** Writing – review & editing, Writing – original draft, Methodology, Investigation, Funding acquisition, Formal analysis, Data curation, Conceptualization. **Leonardo Calderón:** Writing – original draft, Project administration, Methodology, Formal analysis, Data curation. **Chunrong Jia:** Writing – review & editing, Writing – original draft, Methodology, Funding acquisition, Formal analysis. **Hope Davey:** Writing – review & editing, Data curation. **Sanjay Pradeep:** Writing – review & editing, Data curation. **Philip Demokritou:** Writing – review & editing, Writing – original draft, Validation, Supervision, Resources, Project administration, Methodology, Investigation, Funding acquisition, Data curation, Conceptualization.

Declaration of Generative AI and AI-assisted technologies in the writing process

During the preparation of this work the author(s) used ChatGPT in order to review grammar and syntaxis, and to generate the illustration in the graphical abstract. After using this tool/service, the author(s) reviewed and edited the content as needed and take(s) full responsibility for the content of the published article.

Funding

Support for the research reported was provided by UL Research Institutes Grant (Grant 1500496–1), NSF-RAPID (Grant #2524102), NIH/NIEHS (Grant #1R21ES038066–01), NIH/NIEHS (Grant #1R21ES037105–01). Additionally, research was supported by the Rutgers-NIEHS Center for Environmental Exposures and Disease (CEED) (NIH grant # P30ES005022). J.G.C.L. is supported by the Rutgers Presidential Faculty Fellowship and the Harvard JPB Environmental Fellowship Program.

Declaration of Competing Interest

The authors declare that they have no known competing financial interests or personal relationships that could have appeared to influence the work reported in this paper.

Acknowledgement

The financial support to H.D. in part was provided by the Centers for Disease Control and Prevention (CDC)/NIOSH through grant number 5T42OH008412–16 to Southern California Education Research Center, and the Department of Health and Human Services, National Institutes of Health, National Institute of Environmental Health Sciences (NIEHS) through grant number 1R25ES033043–01 to Southern California Superfund Research Program at University of California Los Angeles. Authors acknowledge Emma Landskroner in supporting local sample collection and transportation.

Appendix A. Supporting information

Supplementary data associated with this article can be found in the online version at doi:10.1016/j.jhazmat.2026.142357.

Data Availability

Data will be made available on request.

References

[1] Taccaliti, F., Marzano, R., Bell, T.L., Lingua, E., 2023. Wildland–Urban Interface: Definition and Physical Fire Risk Mitigation Measures, a Systematic Review. Fire 6 (9), 343. https://doi.org/10.3390/fire6090343.
[2] Guo, Y., Wang, J., Ge, Y., Zhou, C., 2024. Global Expansion of Wildland-Urban Interface Intensifies Human Exposure to Wildfire Risk in the 21st Century. Sci Adv 10 (45), eado9587. https://doi.org/10.1126/sciadv.ado9587.
[3] Schug, F., Bar-Massada, A., Carlson, A.R., Cox, H., Hawbaker, T.J., Helmers, D., Hostert, P., Kaim, D., Kasraee, N.K., Martinuzzi, S., Mockrin, M.H., Pfoch, K.A., Radeloff, V.C., 2023. The Global Wildland–Urban Interface. Nature 621 (7977), 94–99. https://doi.org/10.1038/s41586-023-06320-0.
[4] Carlson, A.R., Hawbaker, T.J., Mockrin, M.H., Radeloff, V.C., Bair, L.S., Caggiano, M.D., Meldrum, J.R., Alexandre, P.M., Kramer, H.A., Steblein, P.F., 2025. Rising Rates of Wildfire Building Destruction in the Conterminous United States. Proc Natl Acad Sci USA 122 (51), e2505886122. https://doi.org/10.1073/pnas.2505886122.
[5] Cunningham, C.X., Abatzoglou, J.T., Ellis, T.M., Williamson, G.J., Bowman, D.M.J. S., 2025. Wildfires Will Intensify in the Wildland-Urban Interface under near-Term Warming. Commun Earth Environ 6 (1), 542. https://doi.org/10.1038/s43247-025-02475-y.
[6] Dresser, W.D., Silberstein, J.M., Reid, C.E., Vance, M.E., Wiedinmyer, C., Hannigan, M.P., De Gouw, J.A., 2025. Volatile Organic Compounds Inside Homes Impacted by Smoke from the Marshall Fire. ACS EST Air 2 (1), 4–12. https://doi.org/10.1021/acsestair.4c00259.
[7] Silberstein, J.M., Mael, L.E., Frischmon, C.R., Rieves, E.S., Coffey, E.R., Das, T., Dresser, W., Hatch, A.C., Nath, J., Pliszka, H.O., Reid, C.E., Vance, M.E., Wiedinmyer, C., De Gouw, J.A., Hannigan, M.P., 2023. Residual Impacts of a Wildland Urban Interface Fire on Urban Particulate Matter and Dust: A Study from the Marshall Fire. Air Qual Atmos Health 16 (9), 1839–1850. https://doi.org/10.1007/s11869-023-01376-3.
[8] Hawai'i Department of Health. Lahaina Ash Characterization Testing Show Elevated Levels of Toxic Substances. ⟨https://health.hawaii.gov/news/newsroom/lahaina-ash-characterization-testing-show-elevated-levels-of-toxic-substances/⟩ (accessed 2026-02-17).
[9] Holder, A.L., Ahmed, A., Vukovich, J.M., Rao, V., 2023. Hazardous Air Pollutant Emissions Estimates from Wildfires in the Wildland Urban Interface. PNAS Nexus 2 (6). https://doi.org/10.1093/pnasnexus/pgad186.
[10] Cedeño Laurent, J.G., Parhizkar, H., Calderon, L., Lizonova, D., Tsiodra, I., Mihalopoulos, N., Kavouras, I., Alam, M., Baalousha, M., Bazina, L., Kelesidis, G.A., Demokritou, P., 2024. Physicochemical Characterization of the Particulate Matter in New Jersey/New York City Area, Resulting from the Canadian Quebec Wildfires in June 2023. Environ Sci Technol 58 (33), 14753–14763. https://doi.org/10.1021/acs.est.4c02016.
[11] Singh, D., Tassew, D.D., Nelson, J., Chalbot, M.-C.G., Kavouras, I.G., Demokritou, P., Tesfaigzi, Y., 2022. Development of an Integrated Platform to Assess the Physicochemical and Toxicological Properties of Wood Combustion Particulate Matter. Chem Res Toxicol 35 (9), 1541–1557.
[12] Ghetu, C., Rohlman, D., Smith, B., Scott, R., Adams, K., Hoffman, P., Anderson, K., 2022. Wildfire Impact on Indoor and Outdoor PAH Air Quality. Environ Sci & Technol 56 (14), 10042–10052. https://doi.org/10.1021/acs.est.2c00619.
[13] Verma, V., Polidori, A., Schauer, J.J., Shafer, M.M., Cassee, F.R., Sioutas, C., 2009. Physicochemical and Toxicological Profiles of Particulate Matter in Los Angeles during the October 2007 Southern California Wildfires. Environ Sci & Technol 43 (3), 954–960.
[14] Park, S.S., Harrison, D., Pancras, J.P., Ondov, J.M., 2005. Highly Time-Resolved Organic and Elemental Carbon Measurements at the Baltimore Supersite in 2002. J Geophys Res Atmospheres 110 (D7). https://doi.org/10.1029/2004JD004610.
[15] Molyneux, S., Stec, A.A., Hull, T.R., 2014. The Effect of Gas Phase Flame Retardants on Fire Effluent Toxicity. Polym Degrad Stab 106, 36–46. https://doi.org/10.1016/j.polymdegradstab.2013.09.013.
[16] Jaffe, D.A., O'Neill, S.M., Larkin, N.K., Holder, A.L., Peterson, D.L., Halofsky, J.E., Rappold, A.G., 2020. Wildfire and Prescribed Burning Impacts on Air Quality in the United States. J Air & Waste Manag Assoc 70 (6), 583–615. https://doi.org/10.1080/10962247.2020.1749731.
[17] Boaggio, K., LeDuc, S.D., Rice, R.B., Duffney, P.F., Foley, K.M., Holder, A.L., McDow, S., Weaver, C.P., 2022. Beyond Particulate Matter Mass: Heightened Levels of Lead and Other Pollutants Associated with Destructive Fire Events in California. Environ Sci & Technol 56 (20), 14272–14283.
[18] Blomqvist, P., McNamee, M.S., Stec, A.A., Gylestam, D., Karlsson, D., 2014. Detailed Study of Distribution Patterns of Polycyclic Aromatic Hydrocarbons and Isocyanates under Different Fire Conditions. Fire Mater 38 (1), 125–144. https://doi.org/10.1002/fam.2173.

[19] Tang, W., Emmons, L.K., Wiedinmyer, C., Partha, D.B., Huang, Y., He, C., Zhang, J., Barsanti, K.C., Gaubert, B., Jo, D.S., Zhang, J., Buchholz, R., Tilmes, S., Vitt, F., Granier, C., Worden, H.M., Levelt, P.F., 2025. Disproportionately Large Impacts of Wildland-Urban Interface Fire Emissions on Global Air Quality and Human Health. Sci Adv 11 (11), eadr2616. https://doi.org/10.1126/sciadv.adr2616.
[20] National Academies of Sciences, 2022. Engineering; Medicine (DC). The Chemistry of Fires at the Wildland-Urban Interface. The National Academies Press, Washington. https://doi.org/10.17226/26460.
[21] DeLoid, G.M., Bazina, L., Calderon, L., Kelesidis, G.A., Cedeno Laurent, J.G., Tsiodra, I., Mihalopoulos, N., Fritzky, L., Vaze, N., Xiao, S., Gaskins, A., Demokritou, P., 2026. Wildland-Urban Interface Fires: Toxic Physicochemical Properties of Emitted Particulate Matter and Impacts on Lung Macrophages. Environ Sci Technol. https://doi.org/10.1021/acs.est.5c16340.
[22] Singh, D., Tassew, D.D., Nelson, J., Chalbot, M.-C.G., Kavouras, I.G., Tesfaigzi, Y., Demokritou, P., 2023. Physicochemical and Toxicological Properties of Wood Smoke Particulate Matter as a Function of Wood Species and Combustion Condition. J Hazard Mater 441, 129874. https://doi.org/10.1016/j.jhazmat.2022.129874.
[23] McArdle, C.E., 2023. Asthma-Associated Emergency Department Visits During the Canadian Wildfire Smoke Episodes—United States, April–August 2023. Mmwr Morb Mortal Wkly Rep 72.
[24] Wang, W.; Li, L.; Zhu, Q.; D'Souza, R.R.; Zhang, D.; Zhang, H.; Ebelt, S.; Chang, H. H.; Alonso, A.; Liu, Y. Differential Effects of Wildfire Smoke Fine Particulate Matter Exposure on Respiratory Disease Emergency Department Visits in the Western United States.
[25] Jung, Y.S., Johnson, M.M., Burke, M., Heft-Neal, S., Bondy, M.L., Chinthrajah, R.S., Cullen, M.R., Nelson, L., Dresser, C., Nadeau, K.C., 2025. Fine Particulate Matter From 2020 California Wildfires and Mental Health–Related Emergency Department Visits. JAMA Netw Open 8 (4), e253326. https://doi.org/10.1001/jamanetworkopen.2025.3326.
[26] Chen, H., Samet, J.M., Bromberg, P.A., Tong, H., 2021. Cardiovascular Health Impacts of Wildfire Smoke Exposure. Part Fibre Toxicol 18, 1–22.
[27] Jones, C.G., Rappold, A.G., Vargo, J., Cascio, W.E., Kharrazi, M., McNally, B., Hoshiko, S., 2020. Group, with the C. S. Out-of-hospital Cardiac Arrests and Wildfire-related Particulate Matter during 2015–2017 California Wildfires. J Am Heart Assoc 9 (8), e014125.
[28] Bazina, L., Deloid, G., Fritzky, L., Lizonova, D., Vaze, N., Demokritou, P., 2025. Impact of Canadian Wildfire-Emitted Particulate Matter on THP-1 Lung Macrophage Health and Function. Environ Sci Technol 59 (8), 3869–3883. https://doi.org/10.1021/acs.est.4c10304.
[29] Bazina, L., Deloid, G.M., Calderon, L., Fritzky, L., Vaze, N., Tsiodra, I., Mihalopoulos, N., Pyrsopoulos, T., Demokritou, P., 2026. Impact of Nanoplastics Emitted from Incineration of Polyethylene Plastic on THP-1 Macrophage Viability and Immune Function. J Hazard Mater 501, 140839. https://doi.org/10.1016/j.jhazmat.2025.140839.
[30] Schwarz, L., Frankland, T.B., Tartof, S.Y., Lee, G.S., Gu, Y.M., Mayeda, E.R., González, D.J.X., Benmarhnia, T., Casey, J.A., Chen, C., 2025. Long-Term Exposure to Wildfire Smoke and Mortality: Heterogeneous Effects by Exposure Metric and across Subpopulations. Proc Natl Acad Sci 122 (51), e2509173122. https://doi.org/10.1073/pnas.2509173122.
[31] Jalava, P.I., Salonen, R.O., Hälinen, A.I., Penttinen, P., Pennanen, A.S., Sillanpää, M., Sandell, E., Hillamo, R., Hirvonen, M.-R., 2006. Vitro Inflammatory and Cytotoxic Effects of Size-Segregated Particulate Samples Collected during Long-Range Transport of Wildfire Smoke to Helsinki. Toxicol Appl Pharmacol 215 (3), 341–353. https://doi.org/10.1016/j.taap.2006.03.007.
[32] Hamon, R., Tran, H., Roscioli, E., Ween, M., Jersmann, H., Hodge, S., 2018. Bushfire Smoke Is Pro-Inflammatory and Suppresses Macrophage Phagocytic Function. Sci Rep 8 (1), 1–11. https://doi.org/10.1038/s41598-018-31459-6.
[33] Hansson, A., Rankin, G., Uski, O., Friberg, M., Pourazar, J., Lindgren, R., García-López, N., Boman, C., Sandström, T., Behndig, A., Muala, A., 2023. Reduced Bronchoalveolar Macrophage Phagocytosis and Cytotoxic Effects after Controlled Short-Term Exposure to Wood Smoke in Healthy Humans. Part Fibre Toxicol 20 (1). https://doi.org/10.1186/S12989-023-00541-X.
[34] Kim, Y.H., Warren, S.H., Krantz, Q.T., King, C., Jaskot, R., Preston, W.T., George, B. J., Hays, M.D., Landis, M.S., Higuchi, M., DeMarini, D.M., Gilmour, M.I., 2018. Mutagenicity and Lung Toxicity of Smoldering vs. Flaming Emissions from Various Biomass Fuels: Implications for Health Effects from Wildland Fires. Environ Health Perspect 126 (1), 017011. https://doi.org/10.1289/EHP2200.
[35] Aguilera, R., Corringham, T., Gershunov, A., Benmarhnia, T., 2021. Wildfire Smoke Impacts Respiratory Health More than Fine Particles from Other Sources: Observational Evidence from Southern California. Nat Commun 12 (1), 1493.
[36] Ye, T., Guo, Y., Chen, G., Yue, X., Xu, R., Coêlho, M., de, Saldiva, S.Z.S., Zhao, P.H. N., Li, Q., 2021. S. Risk and Burden of Hospital Admissions Associated with Wildfire-Related PM2· 5 in Brazil, 2000–15: A Nationwide Time-Series Study. Lancet Planet Health 5 (9), e599–e607.
[37] Schollaert, C., Connolly, R., Cushing, L., Jerrett, M., Liu, T., Marlier, M., 2025. Air Quality Impacts of the January 2025 Los Angeles Wildfires: Insights from Public Data Sources. Environ Sci Technol Lett 12 (8), 911–917. https://doi.org/10.1021/acs.estlett.5c00486.
[38] Demokritou, P., Lee, S.J., Ferguson, S.T., Koutrakis, P., 2004. A Compact Multistage (Cascade) Impactor for the Characterization of Atmospheric Aerosols. J Aerosol Sci 35 (3), 281–299. https://doi.org/10.1016/j.jaerosci.2003.09.003.
[39] Tsiodra, I., Grivas, G., Bougiatioti, A., Tavernaraki, K., Parinos, C., Paraskevopoulou, D., Papoutsidaki, K., Tsagkaraki, M., Kozonaki, F.-A., Oikonomou, K., Nenes, A., Mihalopoulos, N., 2024. Source Apportionment of Particle-Bound Polycyclic Aromatic Hydrocarbons (PAHs), Oxygenated PAHs (OPAHs), and Their Associated Long-Term Health Risks in a Major European City. Sci Total Environ 951, 175416. https://doi.org/10.1016/j.scitotenv.2024.175416.
[40] Keith, L.H., 2015. The Source of U.S. EPA's Sixteen PAH Priority Pollutants. Polycycl Aromat Compd 35 (2–4), 147–160. https://doi.org/10.1080/10406638.2014.892886.
[41] Andersson, J.T., Achten, C., 2015. Time to Say Goodbye to the 16 EPA PAHs? Toward an Up-to-Date Use of PACs for Environmental Purposes. Polycycl Aromat Compd 35 (2–4), 330–354. https://doi.org/10.1080/10406638.2014.991042.
[42] Li, T., Su, W., Zhong, L., Liang, W., Feng, X., Zhu, B., Ruan, T., Jiang, G., 2023. An Integrated Workflow Assisted by In Silico Predictions To Expand the List of Priority Polycyclic Aromatic Compounds. Environ Sci Technol 57 (49), 20854–20863. https://doi.org/10.1021/acs.est.3c07087.
[43] Tsiodra, I., Grivas, G., Tavernaraki, K., Paraskevopoulou, D., Parinos, C., Tsagkaraki, M., Liakakou, E., Bougiatioti, A., Gerasopoulos, E., Mihalopoulos, N., 2025. Profiling Aerosol Polycyclic Aromatic Compounds (PACs) in a Severely Polluted European City: A Comprehensive Assessment of the Residential Biomass Burning Impact on Atmospheric Toxicity. J Hazard Mater 494, 138431. https://doi.org/10.1016/j.jhazmat.2025.138431.
[44] Samburova, V., Zielinska, B., Khlystov, A., 2017. Do 16 Polycyclic Aromatic Hydrocarbons Represent PAH Air Toxicity? Toxics 5 (3), 17.
[45] Alam, M., Alshehri, T., Wang, J., Singerling, S.A., Alpers, C.N., Baalousha, M., 2023. Identification and Quantification of Cr, Cu, and As Incidental Nanomaterials Derived from CCA-Treated Wood in Wildland-Urban Interface Fire Ashes. J Hazard Mater 445, 130608.
[46] Baalousha, M., Wang, J., Erfani, M., Goharian, E., 2021. Elemental Fingerprints in Natural Nanomaterials Determined Using SP-ICP-TOF-MS and Clustering Analysis. Sci Total Environ 792, 148426.
[47] Alshehri, T., Wang, J., Singerling, S.A., Gigault, J., Webster, J.P., Matiasek, S.J., Alpers, C.N., Baalousha, M., 2023. Wildland-Urban Interface Fire Ashes as a Major Source of Incidental Nanomaterials. J Hazard Mater 443, 130311. https://doi.org/10.1016/j.jhazmat.2022.130311.
[48] Jia, C., Fu, X., 2017. Diffusive Uptake Rates of Volatile Organic Compounds on Standard ATD Tubes for Environmental and Workplace Applications. Environments 4 (4), 87. https://doi.org/10.3390/environments4040087.
[49] Liu, S., Zhao, S., Liang, Z., Wang, F., Sun, F., Chen, D., 2021. Perfluoroalkyl Substances (PFASs) in Leachate, Fly Ash, and Bottom Ash from Waste Incineration Plants: Implications for the Environmental Release of PFAS. Sci Total Environ 795, 148468. https://doi.org/10.1016/j.scitotenv.2021.148468.
[50] Anjilvel, S., Asgharian, B., 1995. A Multiple-Path Model of Particle Deposition in the Rat Lung. Fundam Appl Toxicol 28 (1), 41–50. https://doi.org/10.1006/faat.1995.1144.
[51] Miller, F.J., Asgharian, B., Schroeter, J.D., Price, O., 2016. Improvements and Additions to the Multiple Path Particle Dosimetry Model. J Aerosol Sci 99, 14–26. https://doi.org/10.1016/j.jaerosci.2016.01.018.
[52] Yeh, H.-C., Schum, G.M., 1980. Models of Human Lung Airways and Their Application to Inhaled Particle Deposition. Bull Math Biol 42 (3), 461–480. https://doi.org/10.1016/S0092-8240(80)80060-7.
[53] Hata, M., Chomanee, J., Thongyen, T., Bao, L., Tekasakul, S., Tekasakul, P., Otani, Y., Furuuchi, M., 2014. Characteristics of Nanoparticles Emitted from Burning of Biomass Fuels. J Environ Sci 26 (9), 1913–1920. https://doi.org/10.1016/j.jes.2014.07.005.
[54] Layshock, J.A., Wilson, G., Anderson, K.A., 2010. Ketone and Quinone-Substituted Polycyclic Aromatic Hydrocarbons in Mussel Tissue, Sediment, Urban Dust, and Diesel Particulate Matrices. Environ Toxicol Chem 29 (11), 2450–2460. https://doi.org/10.1002/etc.301.
[55] Vaze, N., Calderon, L., Tsiodra, I., Mihalopoulos, N., Serhan, C.N., Levy, B.D., Demokritou, P., 2024. Assessment of the Physicochemical Properties of Ultrafine Particles (UFP) from Vehicular Emissions in a Commercial Parking Garage: Potential Health Implications. Toxics 12 (11), 833. https://doi.org/10.3390/toxics12110833.
[56] Azam, N.E., Padhy, P.K., 2025. Analytical Methods for Oxygenated Polycyclic Aromatic Hydrocarbons (OPAHs) in Airborne Particulate: A Review. In: Padhy, P. K., Niyogi, S., Patra, P.K., Hecker, M. (Eds.), Airborne Particulate Matter: Impact on Human Health and Environment. Springer Nature Switzerland, Cham, pp. 61–77. https://doi.org/10.1007/978-3-031-84408-9_5.
[57] Keyte, I.J., Harrison, R.M., Lammel, G., 2013. Chemical Reactivity and Long-Range Transport Potential of Polycyclic Aromatic Hydrocarbons – a Review. Chem Soc Rev 42 (24), 9333. https://doi.org/10.1039/c3cs60147a.
[58] Ringuet, J., Albinet, A., Leoz-Garziandia, E., Budzinski, H., Villenave, E., 2012. Reactivity of Polycyclic Aromatic Compounds (PAHs, NPAHs and OPAHs) Adsorbed on Natural Aerosol Particles Exposed to Atmospheric Oxidants. Atmos Environ 61, 15–22. https://doi.org/10.1016/j.atmosenv.2012.07.025.
[59] Di Filippo, P., Pomata, D., Riccardi, C., Buiarelli, F., Gallo, V., 2015. Oxygenated Polycyclic Aromatic Hydrocarbons in Size-Segregated Urban Aerosol. J Aerosol Sci 87, 126–134. https://doi.org/10.1016/j.jaerosci.2015.05.008.
[60] Allen, J.O., Dookeran, N.M., Taghizadeh, K., Lafleur, A.L., Smith, K.A., Sarofim, A. F., 1997. Measurement of Oxygenated Polycyclic Aromatic Hydrocarbons Associated with a Size-Segregated Urban Aerosol. Environ Sci Technol 31 (7), 2064–2070. https://doi.org/10.1021/es960894g.
[61] Aldekheel, M., Farahani, V.J., Sioutas, C., 2023. Assessing Lifetime Cancer Risk Associated with Population Exposure to PM-Bound PAHs and Carcinogenic Metals in Three Mid-Latitude Metropolitan Cities. Toxics 11 (8), 697. https://doi.org/10.3390/toxics11080697.
[62] McDonald, J.D., Zielinska, B., Fujita, E.M., Sagebiel, J.C., Chow, J.C., Watson, J.G., 2000. Fine Particle and Gaseous Emission Rates from Residential Wood

Combustion. Environ Sci Technol 34 (11), 2080–2091. https://doi.org/10.1021/es9909632.
[63] Tsiodra, I., Georgopoulou, M.P., Florou, K., Kaltsonoudis, C., Parinos, C., Grivas, G., Bougiatioti, A., Pandis, S.N., Mihalopoulos, N., Nenes, A., 2026. Evolution of Polycyclic Aromatic Hydrocarbons (PAHs) and Oxygenated PAHs (OPAHs) in Fresh and Aged Biomass Burning Emissions. Environ Pollut 393, 127654. https://doi.org/10.1016/j.envpol.2026.127654.
[64] Gao, X., Wang, Z., Sun, X., Gao, W., Jiang, W., Wang, X., Zhang, F., Wang, X., Yang, L., Zhou, Y., 2024. Characteristics, Source Apportionment and Health Risks of Indoor and Outdoor Fine Particle-Bound Polycyclic Aromatic Hydrocarbons in Jinan, North China. PeerJ 12, e18553. https://doi.org/10.7717/peerj.18553.
[65] Huang, Q., Xu, M., Zhu, Y., Li, X., Xu, J., Li, X., Lu, Y., 2025. Vehicular Mediated Emissions of Polycyclic Aromatic Hydrocarbons in Roadside Soils of Shanghai. Sci Rep 15 (1), 10981. https://doi.org/10.1038/s41598-025-93715-w.
[66] Hasheminassab, S., Daher, N., Shafer, M.M., Schauer, J.J., Delfino, R.J., Sioutas, C., 2014. Chemical Characterization and Source Apportionment of Indoor and Outdoor Fine Particulate Matter (PM2.5) in Retirement Communities of the Los Angeles Basin. Sci Total Environ 490, 528–537. https://doi.org/10.1016/j.scitotenv.2014.05.044.
[67] Badami, M.M., Aghaei, Y., Sioutas, C., 2025. Impact of Emission Standards on Fine Particulate Matter Toxicity: A Long-Term Analysis in Los Angeles. Toxics 13 (2), 140. https://doi.org/10.3390/toxics13020140.
[68] South Coast Air Quality Management District. 2022 Air Quality Management Plan; Annual Report; South Coast Air Quality Management District: Diamond Bar, CA, 2023. ⟨https://www.aqmd.gov/docs/default-source/air-quality/historical-data-by-year/2023-air-quality-data-tables.pdf?sfvrsn=6⟩ (accessed 2025-11-25).
[69] Teixeira, J., Sousa, G., Azevedo, R., Almeida, A., Delerue-Matos, C., Wang, X., Santos-Silva, A., Rodrigues, F., Oliveira, M., 2024. Characterization of Wildland Firefighters' Exposure to Coarse, Fine, and Ultrafine Particles; Polycyclic Aromatic Hydrocarbons; and Metal(Loid)s, and Estimation of Associated Health Risks. Toxics 12 (6), 422. https://doi.org/10.3390/toxics12060422.
[70] Gill, R.L., Fleck, R., Chau, K., Westerhausen, M.T., Lockwood, T.E., Violi, J.P., Irga, P.J., Doblin, M.A., Torpy, F.R., 2024. Fine Particle Pollution during Megafires Contains Potentially Toxic Elements. Environ Pollut 344, 123306. https://doi.org/10.1016/j.envpol.2024.123306.
[71] Magro, C., Gonçalves, O.C., Nunes, L., Perry, S.H., Rego, F.C., Vieira, P., 2024. Remote Sensing of Volatile Organic Compounds Release during Prescribed Fires in Pine Forests Using Open-Path Fourier Transform Infra-Red Spectroscopy. WF23019 Int J Wildland Fire 33 (4). https://doi.org/10.1071/WF23019.
[72] Marques, B., Kostenidou, E., Valiente, A.M., Vansevenant, B., Sarica, T., Fine, L., Temime-Roussel, B., Tassel, P., Perret, P., Liu, Y., Sartelet, K., Ferronato, C., D'Anna, B., 2022. Detailed Speciation of Non-Methane Volatile Organic Compounds in Exhaust Emissions from Diesel and Gasoline Euro 5 Vehicles Using Online and Offline Measurements. Toxics 10 (4), 184. https://doi.org/10.3390/toxics10040184.
[73] Dickinson, G.N., Miller, D.D., Bajracharya, A., Bruchard, W., Durbin, T.A., McGarry, J.K.P., Moser, E.P., Nuñez, L.A., Pukkila, E.J., Scott, P.S., Sutton, P.J., Johnston, N.A.C., 2022. Health Risk Implications of Volatile Organic Compounds in Wildfire Smoke During the 2019 FIREX-AQ Campaign and Beyond. GeoHealth 6 (8), e2021GH000546. https://doi.org/10.1029/2021GH000546.
[74] Sekimoto, K., Koss, A.R., Gilman, J.B., Selimovic, V., Coggon, M.M., Zarzana, K.J., Yuan, B., Lerner, B.M., Brown, S.S., Warneke, C., Yokelson, R.J., Roberts, J.M., De Gouw, J., 2018. High- and Low-Temperature Pyrolysis Profiles Describe Volatile Organic Compound Emissions from Western US Wildfire Fuels. Atmos Chem Phys 18 (13), 9263–9281. https://doi.org/10.5194/acp-18-9263-2018.
[75] Link, M.F., Davis, A.Y., Lima, N.M., Falkenstein-Smith, R.L., Bryant, R.A., Cleary, T. G., Poppendieck, D., 2025. Wildland-Urban Interface (WUI) Smoke Yields of Nonmethane Organic Gases from Combustion of Small-Scale Residential Building Surrogates. ACS EST Air 2 (11), 2455–2466. https://doi.org/10.1021/acsestair.5c00187.
[76] Urbanski, S.P., 2013. Combustion Efficiency and Emission Factors for Wildfire-Season Fires in Mixed Conifer Forests of the Northern Rocky Mountains, US. Atmos Chem Phys 13 (14), 7241–7262. https://doi.org/10.5194/acp-13-7241-2013.
[77] Yang, B., Shi, Y., Xu, S., Wang, Y., Kong, S., Cai, Z., Wang, J., 2022. Polycyclic Aromatic Hydrocarbon Occurrence in Forest Soils in Response to Fires: A Summary across Sites. Environ Sci Process Impacts 24 (1), 32–41. https://doi.org/10.1039/D1EM00377A.
[78] Tobiszewski, M., Namieśnik, J., 2012. PAH Diagnostic Ratios for the Identification of Pollution Emission Sources. Environ Pollut 162, 110–119. https://doi.org/10.1016/j.envpol.2011.10.025.
[79] Davis, A., Falkenstein-Smith, R., Cleary, T., 2025. Polycyclic Aromatic Hydrocarbons and Select Inorganics in Smoke from Various WUI Fire Fuels: Vehicles, Trees, and Construction Materials. US Department of Commerce, National Institute of Standards and Technology.
[80] Safa, M., O'Carroll, D., Mansouri, N., Robinson, B., Curline, G., 2020. Investigating Arsenic Impact of ACC Treated Timbers in Compost Production (A Case Study in Christchurch, New Zealand). Environ Pollut 262, 114218. https://doi.org/10.1016/j.envpol.2020.114218.
[81] Morrison, J.M., Goldhaber, M.B., Mills, C.T., Breit, G.N., Hooper, R.L., Holloway, J. M., Diehl, S.F., Ranville, J.F., 2015. Weathering and Transport of Chromium and Nickel from Serpentinite in the Coast Range Ophiolite to the Sacramento Valley, California, USA. Appl Geochem 61, 72–86. https://doi.org/10.1016/j.apgeochem.2015.05.018.
[82] Wuana, R.A., Okieimen, F.E., 2011. Heavy Metals in Contaminated Soils: A Review of Sources, Chemistry, Risks and Best Available Strategies for Remediation. Int Sch Res Not 2011 (1), 402647. https://doi.org/10.5402/2011/402647.
[83] Klöckner, P., Reemtsma, T., Eisentraut, P., Braun, U., Ruhl, A.S., Wagner, S., 2019. Tire and Road Wear Particles in Road Environment – Quantification and Assessment of Particle Dynamics by Zn Determination after Density Separation. Chemosphere 222, 714–721. https://doi.org/10.1016/j.chemosphere.2019.01.176.
[84] Funari, V., Bokhari, S.N.H., Vigliotti, L., Meisel, T., Braga, R., 2016. The Rare Earth Elements in Municipal Solid Waste Incinerators Ash and Promising Tools for Their Prospecting. J Hazard Mater 301, 471–479. https://doi.org/10.1016/j.jhazmat.2015.09.015.
[85] Glüge, J., Scheringer, M., Cousins, I.T., DeWitt, J.C., Goldenman, G., Herzke, D., Lohmann, R., Ng, C.A., Trier, X., Wang, Z., 2020. An Overview of the Uses of Per- and Polyfluoroalkyl Substances (PFAS). Environ Sci Process Impacts 22 (12), 2345–2373. https://doi.org/10.1039/D0EM00291G.
[86] Moody, C.A., Field, J.A., 2000. Perfluorinated Surfactants and the Environmental Implications of Their Use in Fire-Fighting Foams. Environ Sci Technol 34 (18), 3864–3870. https://doi.org/10.1021/es991359u.
[87] Interstate Technology & Regulatory Council. Per- and Polyfluoroalkyl Substances (PFAS) Technical and Regulatory Guidance Document; ITRC PFAS-1; Interstate Technology & Regulatory Council, 2020. ⟨https://downloads.regulations.gov/EPA-HQ-OW-2021-0547-0369/content.pdf⟩.
[88] United States Environmental Protection Agency. Multi-Industry Per- and Polyfluoroalkyl Substances (PFAS) Study – 2021 Preliminary Report; EPA-821-R-21-004; U.S. Environmental Protection Agency, Office of Water: Washington, DC, 2021. ⟨https://www.epa.gov/system/files/documents/2021-09/multi-industry-pfas-study_preliminary-2021-report_508_2021.09.08.pdf⟩.
[89] Buck, R.C., Franklin, J., Berger, U., Conder, J.M., Cousins, I.T., de Voogt, P., Jensen, A.A., Kannan, K., Mabury, S.A., van Leeuwen, S.P., 2011. Perfluoroalkyl and Polyfluoroalkyl Substances in the Environment: Terminology, Classification, and Origins. Integr Environ Assess Manag 7 (4), 513–541. https://doi.org/10.1002/ieam.258.
[90] Adachi, K., Dibb, J.E., Scheuer, E., Katich, J.M., Schwarz, J.P., Perring, A.E., Mediavilla, B., Guo, H., Campuzano-Jost, P., Jimenez, J.L., Crawford, J., Soja, A.J., Oshima, N., Kajino, M., Kinase, T., Kleinman, L., Sedlacek, I.I.I., Yokelson, A.J., Buseck, R.J., 2022. P. R. Fine Ash-Bearing Particles as a Major Aerosol Component in Biomass Burning Smoke. J Geophys Res Atmospheres 127 (2), e2021JD035657. https://doi.org/10.1029/2021JD035657.
[91] Bodí, M.B., Martin, D.A., Balfour, V.N., Santín, C., Doerr, S.H., Pereira, P., Cerdà, A., Mataix-Solera, J., 2014. Wildland Fire Ash: Production, Composition and Eco-Hydro-Geomorphic Effects. Earth-Sci Rev 130, 103–127. https://doi.org/10.1016/j.earscirev.2013.12.007.
[92] Kajita, E., Chang, K., De Leon, V., Moss, W., Lim, M., Balter, S., De St. Maurice, A., 2025. *Notes from the Field:* Emergency Department Use During the Los Angeles County Wildfires, January 2025. MMWR Morb Mortal Wkly Rep 74 (3), 40–42. https://doi.org/10.15585/mmwr.mm7403a2.
[93] Weichenthal, S., Christidis, T., Olaniyan, T., Van Donkelaar, A., Martin, R., Tjepkema, M., Burnett, R.T., Brauer, M., 2024. Epidemiological Studies Likely Need to Consider PM2.5 Composition Even If Total Outdoor PM2.5 Mass Concentration Is the Exposure of Interest. Environ Epidemiol 8 (4), e317. https://doi.org/10.1097/EE9.0000000000000317.